

Desorption of organic overlayers by Ga and C₆₀ bombardment

B. Czerwiński^a, R. Samson^a, B.J. Garrison^b, N. Winograd^b, Z. Postawa^{a,*}

^aSmoluchowski Institute of Physics, Jagellonian University, ul. Reymonta 4, 30 059 Krakow 16, Poland

^bDepartment of Chemistry, The Pennsylvania State University, University Park, PA 16802, USA

Abstract

This paper reviews our recent work on computer simulations of Ga and C₆₀ bombardment of thin organic overlayers deposited on metal substrate. A multilayer of benzene, a monolayer of PS4 on Ag{1 1 1} and a self-assembled monolayer of octanethiol molecules on Au{1 1 1} were irradiated with 15 keV monoatomic (Ga) and polyatomic (C₆₀) projectiles that are recognized as valuable sources for desorption of high mass particles in secondary ion and neutral mass spectrometry (SIMS/SNMS) experiments. The results indicate that the sputtering yield decreases with the increase of the binding energy and the average kinetic energy of parent molecules is shifted toward higher kinetic energy. Although the total sputtering yield of organic material is larger for 15 keV C₆₀, the impact of this projectile leads to a significant fragmentation of ejected species. As a result, the yield of the intact molecules is comparable for C₆₀ and Ga projectiles. Our results indicate that the chemical analysis of thin organic films performed by detection of sputtered neutrals will not benefit from the use of C₆₀ projectiles.

© 2006 Elsevier Ltd. All rights reserved.

Keywords: Sputtering; Cluster bombardment; Organic overlayers; SIMS/SNMS; Molecular dynamics computer simulations

1. Introduction

The impact of an energetic ion on a metallic substrate covered with an organic overlayer triggers a chain of events that finally leads to the ejection of both substrate atoms and adsorbate molecules. Understanding of these complex phenomena is not only of fundamental interest, but also could allow for the development of improved detection strategies for molecular surface characterization based on ion beam desorption techniques. Cluster ion beams are recognized as valuable sources for desorption of high mass ions in time-of-flight secondary ion mass spectrometry (TOF-SIMS) experiments [1,2]. For instance, the yield of the peptide gramicidin parent ion is enhanced by a factor of 1300 during C₆₀⁺ impact when compared to Ga⁺ ion bombardment [3]. There is also a plethora of recent experimental observations that indicate that C₆₀ projectiles can be very useful for imaging TOF-SIMS applications [2,4].

The reasons behind the unique properties of cluster ion beams are still not well understood. Various degrees of enhancement of high mass secondary ions have been reported, depending upon the type of projectile, target material and matrix [5]. For example, thin polymer films on Ag do not seem to benefit from the use of polyatomic projectiles, while SIMS spectra from bulk polymers are dramatically improved [5]. Theoretical calculations are beginning to unravel some of the phenomena responsible for cluster-induced sample erosion [2,6–16]. The molecular dynamics (MD) simulations of C₆₀ impact with kinetic energies in range of 10–20 keV on graphite [11,12] and diamond [13] show that a crater forms and that the energy is deposited in the near surface region. Calculations of small metal cluster bombardment in the same energy range predict similar crater formation on graphite and metal substrates [7–10,16]. At lower kinetic energies, it has been shown that the mass of the substrate is important in determining the mechanism of the enhancement effect [14].

To understand the signal enhancement in TOF-SIMS experiments and to predict optimal experimental configurations, we have initiated a comprehensive series of MD investigations aimed toward understanding collision

*Corresponding author. Tel.: +48 12 632 48 88; fax: +48 12 632 70 86.
E-mail address: zp@castor.if.uj.edu.pl (Z. Postawa).

cascades initiated by a keV C_{60} cluster bombardment [17–20]. The strategy involves utilizing well-defined model substrates to elucidate how the atomic motion and subsequent measurable quantities depend upon the nature of the incident particle, either an atomic species such as Ga or the cluster C_{60} . In our previous studies we have found that the C_{60} projectile has several advantages as compared to Ga when used to analyze metallic samples [17,18]. Cluster bombardment can greatly enhance the yield over the atomic irradiation. The damage created by C_{60} is much more confined than that induced by Ga. And finally, C_{60} causes lower effective beam-induced contamination and leads to smaller surface roughening. The predictions from these calculations have compared favorably to the experimental data [2,4]. In this paper we review the results of the study of sputtering of thin organic overlayers deposited on metal substrates by 15 keV Ga and C_{60} projectiles. A thin layer of C_6H_6 [19], a monolayer of polystyrene tetramers (PS4) on the $Ag\{111\}$ [20] and a self-assembled monolayer (SAM) of the octanethiol ($CH_3(CH_2)_7SH$) on the $Au\{111\}$ surface are selected to represent both physisorbed and chemisorbed molecules.

2. Model

MD computer simulations have been used to elucidate the differences between Ga and C_{60} bombardment of thin organic overlayers. The details of simulations can be found elsewhere [21]. Briefly, the motion of the particles is determined by integrating Hamilton's equations of motion. The forces among the atoms are described by a blend of empirical pair-wise additive and many-body potential energy functions. The Ag–Ag and Au–Au interactions are described by the molecular dynamics/Monte Carlo corrected effective medium (MD/MC-CEM) potential for fcc metals [22]. The interactions with Ga atom are described using the purely repulsive Molière pair-wise additive potential. The adaptive intermolecular potential, AIREBO, developed by Stuart and coworkers is used to describe the hydrocarbon interactions [23]. The interaction of C and H atoms with Ag and Au as well as the H–S interaction is described by a Lennard-Jones potential using established parameters [19,24]. The S–S and S–C interactions are described by Morse potential [24]. For the particular case of the Au–S bond, height-dependent modified Morse potential is used to better describe the Au-thiolate clusters [24].

The model approximating the $Ag\{111\}$ and $Au\{111\}$ substrates consists of a finite microcrystallite containing 166 530 atoms arranged in 39 layers of 4270 atoms each. The sample size was chosen to minimize edge effects associated with the dynamical events leading to ejection of particles. Organic overlayers are represented by a three layers of benzene [19], a monolayer of sec-butyl-terminated polystyrene tetramers (PS4) adsorbed on an $Ag\{111\}$ [20] and a self-assembled monolayer (SAM) of octanethiol molecules ($CH_3(CH_2)_7S$) adsorbed on the 3-fold sites of the

$Au\{111\}$ in a $\sqrt{3}x\sqrt{3} - R30^\circ$ arrangement. The adsorption scheme and the potential parameters for thiol molecules were adopted from Ref. [24], however, the crystallite size was significantly enlarged to contain more energetic processes induced by 15 keV projectiles. In all the considered systems, the mass of hydrogen is taken to be that of tritium (3 amu) to increase computational efficiency. The mass of the C_6H_6 is 90, the mass of PS4 is 559 amu and the mass of octanethiol is 179 instead of 78, 474 and 145 amu, respectively. Prior to projectile impact, the entire system is relaxed to a minimum energy configuration. This procedure yields the resulting binding energy of 1.8 eV for thiol and 2.1 eV for polystyrene tetramer, which is several times larger than the binding energy of adsorbed benzene overlayer (~ 0.4 eV). Both PS4 and benzene are physisorbed to an $Ag\{111\}$. The high binding energy of PS4 is achieved by cumulative interaction of this molecule at multiple contact points with the surface. On the other hand, octanethiol molecules chemisorb to Au. During this process the S–H bond is replaced by a stronger S–Au bond and the molecule is attached to the surface by a single contact point.

The atoms in the target initially have zero velocity. The atoms in the C_{60} projectile initially have no velocity relative to the center of mass motion. The trajectory is terminated when the total energy of the most energetic particle remaining in the solid is less than 0.05 eV. The time of each trajectory ranges between 9 and 15 ps and depends upon the type of primary projectile, its impact point and the manner in which the energy distributes within the solid. A special care was taken to eliminate the artifacts associated with generation of the pressure waves by the C_{60} bombardment as described in [17].

3. Results and discussion

Snapshots of the temporal evolution of typical collision events leading to ejection of particles due to 15 keV Ga and C_{60} bombardment of 3 layer C_6H_6 system on $Ag\{111\}$ are shown in Fig. 1. A significant portion of the benzene overlayer is altered upon the impact of either projectile. The nature of the collision events leading to these changes, however, is different for Ga and C_{60} . The Ga projectile easily penetrates through the organic overlayer losing, on average, only ~ 0.4 keV of the initial 15 keV. Direct collisions between Ga and benzene molecules lead to the formation of a small number of energetic organic fragments. After passing through the organic overlayer, the Ga projectile penetrates into the substrate depositing most of its kinetic energy at a considerable depth similar to the motion induced without the overlayer [17,18]. The energy is subsequently redistributed within the crystal and a highly excited cylindrical volume is formed. Only a small portion of the primary energy is deposited near the Ag surface leading to ejection of substrate particles. These upward moving Ag particles collide with the C_6H_6

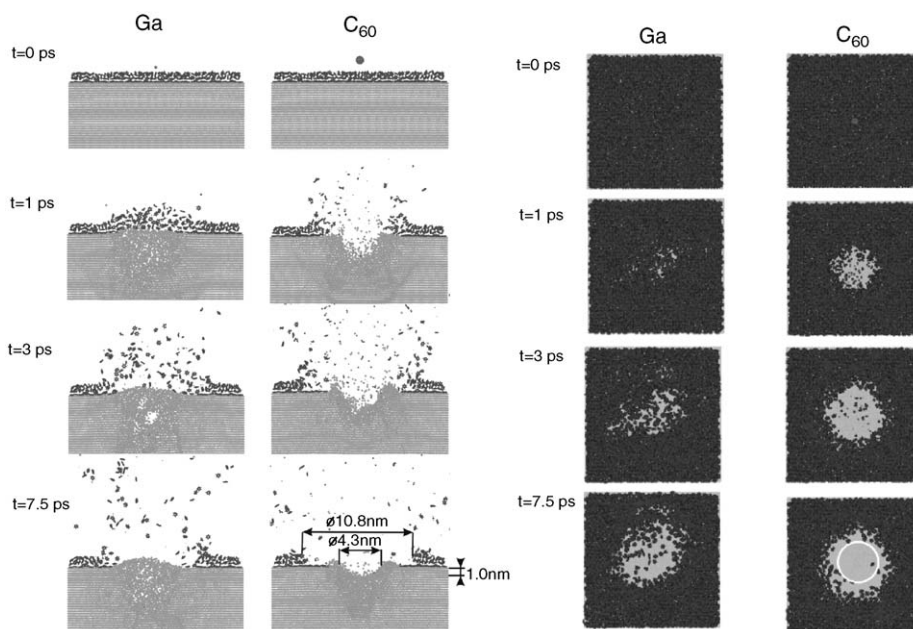


Fig. 1. A cross-sectional view and top view of the temporal evolution of a typical collision event leading to ejection of particles due to 15 keV Ga and C₆₀ bombardment at normal incidence of a 3 layer benzene system deposited upon a Ag{111} surface [19]. The dimensions shown on the 7.5 ps snapshot of the C₆₀ bombardment is for the depth and width of the Ag crater and the swept-out region of the benzene overlayer. A slice 1.5 nm wide in the center of the system is shown. The white circle denotes the outer rim of the crater formed in the Ag substrate by C₆₀ impact

molecules located above them, leading to ejection of molecules and fragments.

Ejection of Ag atoms induced by 15 keV Ga occurs in a relatively short time. For instance, most of ejection events occur within 1.7 ps for the clean Ag system [17,18]. Even after 1.7 ps, however, there is still considerable disruption in the substrate as evidenced by the cavity apparent in the 3 ps snapshot in Fig. 1. Due to the subsurface collision cascade, there is a correlated upward motion of Ag atoms towards the surface [25]. The energy involved in this process is low but it is sufficient to eject the remaining portion of the loosely bound benzene overlayer as shown in the 3 ps frame. The final configuration has most of the C₆H₆ molecules in the region where the Ga particle struck the surface removed. Similar phenomena are observed for PS4 and octanethiol overlayers. However, due to a much larger binding energy of these molecules the ejection process terminates earlier. Also the correlated upward motion of substrate atoms during formation of the bulged surface is not sufficiently energetic to uplift strongly bound molecules. In result, the amount of removed organic material is lower and the extent of the damage induced by the Ga projectile in the organic overlayer is smaller than for benzene [20].

As seen in Fig. 2(a) the process of the energy transfer between the Ga projectile and the sample atoms can be visualized as a chain of subsequent collisions. In this case, there is a great diversity of the types of motion that can occur [26]. One way of representing this diversity is to plot the number of organic molecules that will be removed from the surface by a subsequent projectile impact. Shown in

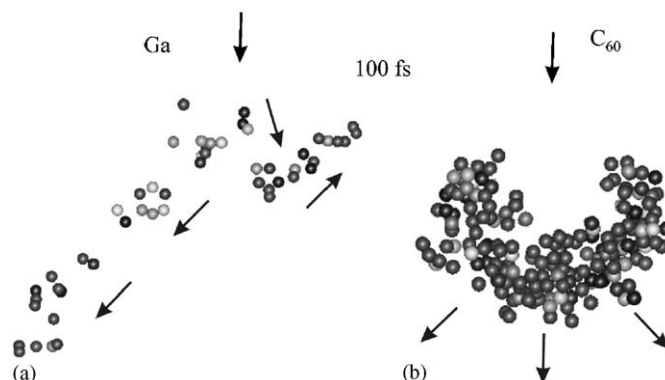


Fig. 2. The evolution of the collision cascade due to (a) 15 keV Ga and (b) 15 keV C₆₀ bombardment of a clean Ag{111} surface. The snapshots were taken at 100 fs after the projectile impact and represent a slice 0.8 nm wide centered at the impact point of the projectile. Only the particles with a kinetic energy larger than 1 eV are shown.

Fig. 3(a) is such a distribution for 15 keV Ga bombardment of C₆H₆/Ag{111} system. There is a wide spread in the number of removed molecules from almost zero to almost 500 with an average yield, S_{tot} , of 227. It is obvious from this figure that there are numerous trajectories that are wasted in terms of providing a useful signal for SIMS/SNMS applications.

A different scenario takes place during C₆₀ impact. Due to its large size C₆₀ interacts strongly with the sample atoms. As shown in Fig. 2(b) the process is almost mesoscopic in a sense that the interaction of a C₆₀ projectile with the rest of the system is a many body collision in which several projectile atoms simultaneously

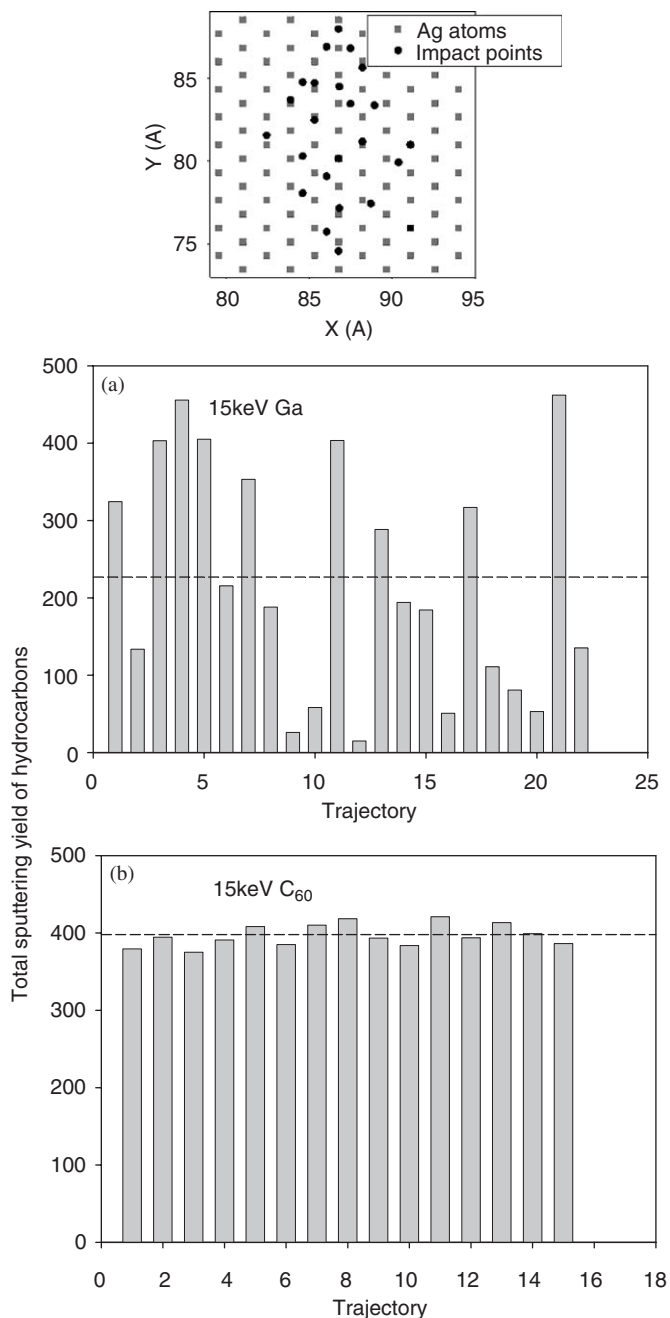


Fig. 3. The distribution of the total sputtering yield of benzene ejected from a benzene overlayer bombarded by (a) 15 keV Ga and (b) 15 keV C_{60} projectiles at normal incidence. The selected impact points are shown at the top as dark circles superimposed on the position of substrate silver atoms (gray squares). The positions of C and H atoms are not shown for clarity. The average sputtering yields are depicted by a broken line.

hit the same target atom. The individual atoms in the cluster are not initiating their own collision cascades; rather they are working cooperatively to move the target atoms. One of the consequences of such activity is generation of pressure waves that propagate both in the substrate and in the loosely bound organic overlayer. As opposed to the atomic projectile, the C_{60} interacts strongly with the benzene overlayer. On average, 8.8 keV of the initial kinetic

energy is deposited into the benzene overlayer by the 15 keV C_{60} projectile. The main portion of this energy is used to create a large number of molecular fragments [19]. A part of this energy is also used to generate a planar pressure wave that propagates in the overlayer pushing the benzene molecules aside from the point of impact [19].

After impact of the C_{60} projectile on the Ag substrate the spatial correlation of C atom movements is lost. Due to the heavier mass of the substrate Ag atoms, most of the C atoms originating from the projectile are reflected towards the organic overlayer. Consequently, the energy of the cluster projectile is deposited in a shallow volume of the substrate in a short time leading to the ejection of many substrate particles. As a result a crater is formed. Since a significant portion of the primary kinetic energy is dissipated during penetration of the organic overlayer, the size of the crater formed in the substrate is significantly smaller than the crater for clean Ag{111} [18]. This crater formation leads to a temporally and spatially correlated motion of metal substrate particles as shown in Fig. 1 at about 3 ps. The average kinetic energy of atoms taking part in this process is larger than for atoms involved in the formation of the bulge during Ga bombardment. These particles collectively interact with adsorbed organic molecules, uplifting most of the remaining molecules in this area. The unfolding of the crater acts as a sling or catapult that hurls the organic molecules into the vacuum. We find that this mechanism is mainly responsible for ejection of intact organic molecules from C_{60} -irradiated organic overlayers [19,20].

The mesoscopic character of the C_{60} bombardment can be also observed in Fig. 3(b). In contrary to the Ga bombardment, the removal of organic material is almost independent of the impact point. This is a very fortunate property from the point of view of the computer modeling because it indicates that just a few sample trajectories are sufficient to fully characterize all processes taking place during C_{60} bombardment of organic overlayers. There is high action on every impact and there are no longer incident projectiles that eject little material. The ability of removing similar amount of material by the analyzing projectile is also important from the practical point of view. For instance, it will allow to achieve a uniformity of information throughout the scanning process in imaging SIMS/SNMS applications [4]. Again, similar processes are observed for PS4/Ag{111} and octanethiol/Au{111} systems. As for Ga bombardment, the signal is lower due to higher binding energy of the molecular film. There are, however, some interesting differences. First, the energy loss in the PS4 overlayer is minimal (<0.5 keV) as the projectile easily penetrates very thin and open monolayer. This leads to a formation of a larger crater and to an alteration of a significant portion of the investigated organic overlayer. On the other hand, the energy loss in a thicker and much denser octanethiol layer is even larger (~ 10 keV) than for benzene. In result, the contribution of organic fragments in the total organic flux is the largest for this overlayer.

Table 1

Number of particles ejected from a multilayer $C_6H_6/Ag\{111\}$, a monolayer $PS4/Ag\{111\}$ and a self-assembled monolayer of octanethiol deposited at $Au\{111\}$ systems bombarded by 15 keV Ga and C_{60} projectiles at normal incidence at 15 ps after the projectile impact

Particle	Projectile					
	Benzene		PS4		Octanethiol	
	Ga	C_{60}	Ga	C_{60}	Ga	C_{60}
Total Ag yield	15	81	14	229		
Total Au yield					19.4	59
Total organic yield	227	398	7.5	12	8.5	70
Intact organic molecules	120	244	5.8	4.7	0.5	0.5
Organic molecules in smaller clusters and fragments	8.5	82	0.1	4.0	4.1	53.5
Organic molecules in larger clusters	99	75	1.2	1.1	3.7	16

The yields for organic species are given in number of ejected benzene, PS4 and octanethiol molecules, respectively.

Finally, the animations of the sputtering events indicate that there is no pressure wave propagating in the PS4 system. The stronger binding energy and/or larger intermolecular separation can be responsible for the lack of this phenomenon. Propagation of some pressure wave is observed at the C_{60} -irradiated octanethiol overlayer but the energy transferred by the wave is too low to relocate strongly bound molecules.

The sputtering yields of molecules ejected from investigated organic systems bombarded with 15 keV Ga and 15 keV C_{60} projectiles at normal incidence are shown in Table 1. Emission of intact C_6H_6 and PS4 molecules composes a significant portion of the sputtered flux from the Ga-irradiated benzene and PS4 overlayers, whereas only a very minor ejection of intact molecules is observed from the octanethiol overlayer. Substrate particles and small hydrocarbon fragments compose a majority of ejectees from the C_{60} -irradiated samples. For instance, 81 and 59 substrate atoms are ejected from $C_6H_6/Ag\{111\}$ and octanethiol/ $Au\{111\}$ systems and almost 230 atoms are ejected from $PS4/Ag\{111\}$. Two processes can influence ejection of substrate particles. First, the energy of the projectile deposited in the organic overlayer will not contribute to the ejection of substrate atoms. Second, ejecting substrate particles can be blocked by higher lying organic molecules. We believe that the first process plays the major role for C_{60} bombardment. This would explain why there are much more silver atoms ejected from a thin and open PS4 system. If blocking of ejecting substrate particles was the most important process one would expect to see a larger ejection from the Ga-bombarded $PS4/Ag\{111\}$ system than from benzene-covered Ag crystal. As it is evident from Table 1 this is not the case because almost the same number of substrate atoms is ejected from both systems.

The number of ejected intact benzene molecules is larger for the C_{60} projectile than for the Ga projectile. However, this observation is no longer valid for PS4 and octanethiol overlayers. In these cases the number of ejected intact molecules is in fact smaller or comparable for the 15 keV C_{60} projectile than for 15 keV Ga. Such behavior is a bit

unexpected especially that the total sputtering yield of organic material from these overlayers is still larger for C_{60} than for Ga. In fact, the difference can be quite large and, for instance, the C_{60} projectile can be 10 times more efficient in removing of organic material from a dense octanethiol overlayer. Unfortunately, most of this enhancement is caused by ejection of molecular fragments at the early stages of sputtering when energetic and large C_{60} cluster penetrates the overlayer.

The data shown in Table 1 are not corrected for a possible post-ejection unimolecular decomposition of molecules and clusters on their way to the detector. Unimolecular decomposition theory predicts that more than 90% of C_6H_6 and PS4 molecules will be detected on a μs time scale if their internal energy does not exceed 4.6 and 28 eV, respectively [26]. Our calculations indicate that more internally excited molecules are ejected by C_{60} irradiation of thin organic overlayers [20]. For instance, approximately 9% C_6H_6 and 5% of PS4 molecules have an internal energy higher than the assumed dissociation thresholds for Ga projectile bombardment. At the same time, $\sim 21\%$ of C_6H_6 and $\sim 14\%$ of PS4 molecules ejected by C_{60} impact have internal energies exceeding the threshold values. All of these molecules will dissociate and, consequently, they would not be detected experimentally. Because of the decrease in the yields of intact molecules due to dissociation, the final enhancement factor in the useful signal will, therefore, be even smaller than calculated from the data presented in Table 1.

The kinetic energy distribution of ejected particles is a quantity that can be measured and, at times, can be used to help understand the mechanisms responsible for emission. Angle-integrated kinetic energy distributions of C_6H_6 and PS4 molecules ejected due to 15 keV Ga and C_{60} projectiles are displayed in Fig. 4. The distribution of octanethiol molecules is not shown because it was too noisy due to a limited number of currently probed trajectories. The kinetic energy distributions are consistent with the picture in which more energetic processes are involved in ejection of organic molecules due to C_{60} bombardment vs. Ga bombardment. In addition, it is obvious that there is a

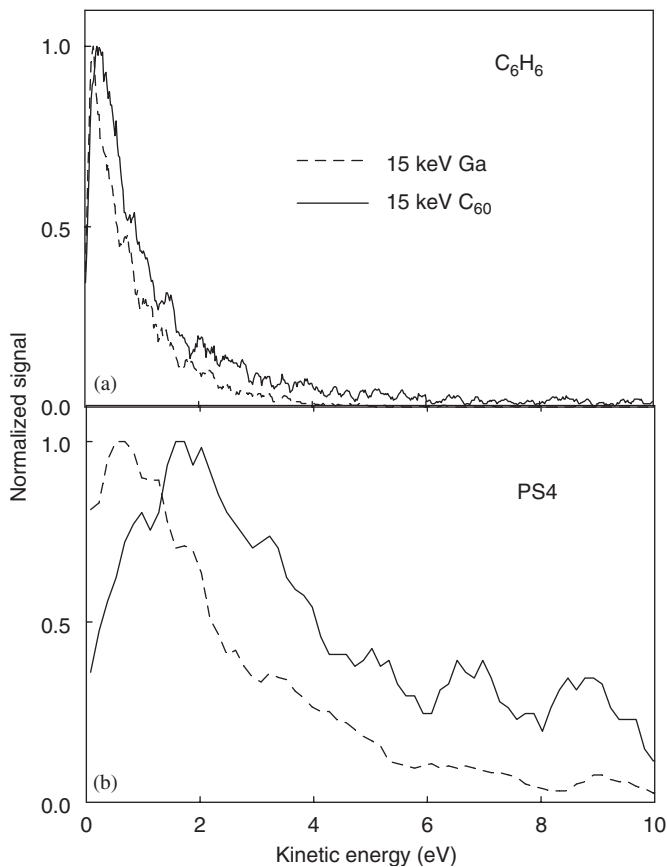


Fig. 4. Peak normalized kinetic energy distributions of (a) C_6H_6 and (b) PS4 molecules sputtered at normal incidence from $Ag\{111\}$ by 15 keV Ga (broken) and C_{60} (solid line).

correlation between the most probable kinetic energy and the binding energy of the molecules as more strongly bound PS4 molecules are ejected with higher kinetic energy.

The mechanistic analysis of the sputtering process indicates that intact molecules are ejected during C_{60} irradiation by a concerted action of Ag atoms involved in the unfolding of the crater [19,20]. The motion of these atoms is spatially and temporally correlated and they have a relatively low kinetic energy. The unfolding of the crater acts as a sling or catapult that hurls the organic molecules into the vacuum. This ejection mechanism should have a visible effect on the angular characteristics of molecular emission. Indeed, as presented in Fig. 5, ejection of intact C_6H_6 and PS4 molecules by C_{60} impact exhibits a distinct ring-like structure that mimics the geometry of the underlying crater. The ejection is azimuthally isotropic and peaks at a polar angle of approximately 40° for benzene and 45° for PS4 with respect to the surface normal. The azimuthal isotropy is also observed in the angular distributions of intact molecules ejected by Ga impact but, in this case, the emission peaks along the normal to the surface.

Up to this point the ejection of molecules from thin organic overlayers was discussed. The experimental measurements indicate that the behavior of thick organic

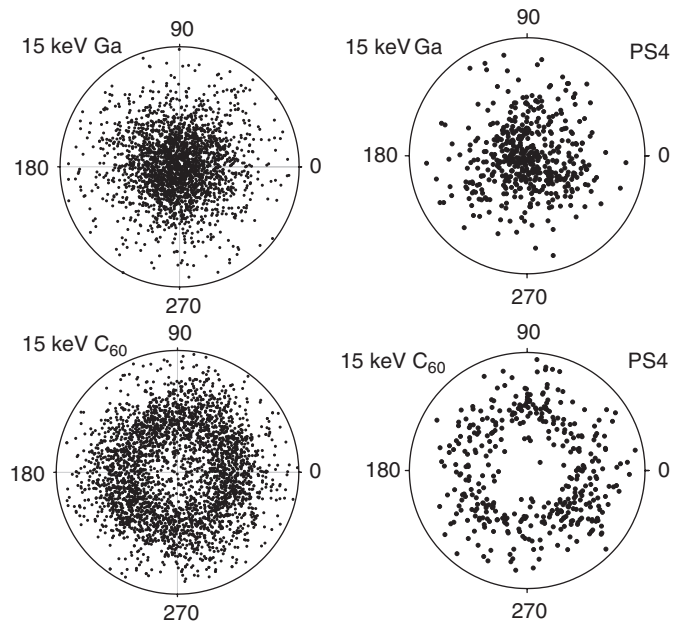


Fig. 5. Angular distribution of C_6H_6 (left) and PS4 (right) molecules ejected by 15 keV Ga (top) and 15 keV C_{60} (bottom) bombardment at normal incidence. The data are presented for deposition on a flat plate collector located 3 cm in front of the surface.

materials bombarded with atomic and cluster ions can be quite different [2,4,6]. We have initiated calculations on a thick benzene crystal. Although, this microcrystal contained 24 840 molecules it was way too small to contain the primary energy of 15 keV projectiles. For this reason we had to reduce the kinetic energy of the projectile to 500 eV. Even at this low kinetic energy the calculations were found to be extremely time consuming due to complicated many-body potentials used to describe hydrocarbon interactions. Almost 6 months were needed to complete a single trajectory for both 500 eV C_{60} and Ga. One conclusion from these limited calculations was that the difference between the penetration depths of these two projectiles is much larger than observed on metal samples. Although the energy of C_{60} cluster was still deposited close to the surface, Ga projectile penetrated deep into the sample. In result, one may expect to observe a more pronounced difference in the sputtering yields stimulated by C_{60} projectiles, preferring this ion as a more efficient molecular lifter. However, the enormous amount of time required to complete these calculations makes this approach impractical, at least using currently available hardware. It has been proposed, however, that the computational effort can be significantly reduced by grouping several atoms or molecules into one particle and by selecting pair-wise potentials to describe interactions within this simplified system. These united atom or coarse-grained approaches have been successful for modeling of a number of phenomena including self-assembled monolayers on metal substrates [27] and laser ablation of molecular solids [28,29]. The advantages of these coarse-grained approaches are that there are fewer particles, the potentials are simpler

thus faster to calculate and the annoying H-vibration is eliminated which allows for a larger time step to be used in the integration. We have made some preliminary calculations on a thick benzene sample adopting this approach [30]. The first results are very promising and show that we can properly reproduce both the total sputtering yield and the extent of damage induced by impinging projectiles obtained in our full atomistic simulations. It is fascinating that only couple days, instead of months, were needed to complete the calculations. Therefore, we believe that the coarse-grained approach will open the door for a modeling of very large organic systems bombarded by high-energy projectiles.

4. Conclusion

Impact of Ga projectile initiates a sequence of collisions that lead to the ejection of organic molecules whereas more collective, almost mesoscopic process is initiated by the impact of C_{60} ion. Most of sputtered intact molecules are emitted due to processes initiated in the metallic substrate. The energy deposited directly by a projectile in the organic overlayer leads predominantly to the emission of molecular fragments. In systems bombarded by atomic projectiles the organic molecules are uplifted by collisions with departing substrate atoms. The intact molecules are ejected during C_{60} irradiation by a concerted action of substrate atoms involved in the unfolding of the crater. The motion of these atoms is spatially and temporally correlated and they have a relatively low kinetic energy. The unfolding of the crater acts as a sling or catapult that hurls the organic molecules into the vacuum.

The presented data indicate that there is no gain in application of C_{60} projectiles in chemical analysis of benzene, PS4 and octanethiol thin overlayers. Although emission of substrate particles is significantly enhanced, there is little to no enhancement of the ejection of intact molecules and the mass spectrum contains more molecular fragments. This conclusion agrees with experimental observations reported by Kotter and Benninghoven of bombardment of thin polystyrene layers [5]. Several factors can be responsible for such behavior. First, in weakly bound thin organic layers there is a limited number of physisorbed organic molecules available for desorption and the processes taking place after Ga and C_{60} impact are energetic enough to desorb most of the adsorbed molecules. In addition, in these systems the impact of the C_{60} projectile generates a pressure wave that propagates in the organic overlayer pushing the molecules away from the point of impact. As a result, these molecules avoid collisions with ejecting substrate particles and are unable to eject. The same phenomenon is not observed or inefficient for more strongly bound PS4 or octanethiol overlayers. In this case, however, the fragmentation of molecules plays a significant role in reducing the efficiency

of molecular ejection. We find that almost half of all removed PS4 and almost all octanethiol molecules are fragmented.

Acknowledgments

The financial support from the Polish Committee for Scientific Research program no. 3T09A12426, Rector of the Jagiellonian University and the National Science Foundation are gratefully acknowledged.

References

- [1] Castner DG. *Nature* 2003;422:129 and references therein.
- [2] Winograd N. *Anal Chem* 2005;77:142A and references therein.
- [3] Weibel D, Wong S, Lockyer N, Blenkinsopp P, Hill R, Vickerman JC. *Anal Chem* 2003;75:1754.
- [4] Winograd N, Postawa Z, Cheng J, Szakal Ch, Kozole J, Garrison BJ. *Appl Surf Sci* and references therein, in press.
- [5] Kotter F, Benninghoven A. *Appl Surf Sci* 1998;133:47.
- [6] Postawa Z. *Appl Surf Sci* 2004;231–232:22 and references therein.
- [7] Haberland H, Isepov Z, Moseler M. *Phys Rev B* 1995;51:11061.
- [8] Webb RP, Kerford M, Way A, Wilson I. *Nucl Instrum Methods B* 1999;153:284.
- [9] Colla ThJ, Aderjan R, Kissel R, Urbassek HM. *Phys Rev B* 2000;62:8487.
- [10] Aderjan R, Urbassek HM. *Nucl Instrum Methods B* 2000;164:697.
- [11] Kerford M, Webb RP. *Nucl Instrum Methods B* 2001;180:44.
- [12] Seki T, Aoki T, Tanomura M, Matsuo J, Yamada I. *Mater Chem Phys* 1998;54:143.
- [13] Aoki T, Seki T, Matsuo J, Insepov Z, Yamada I. *Mater Chem Phys* 1998;54:139.
- [14] Nguyen TC, Ward DW, Townes JA, White AK, Krantzman KD, Garrison BJ. *J Phys Chem B* 2000;104:8221.
- [15] Anders Ch, Urbassek HM, Johnson RR. *Phys Rev B* 2004;70:155404.
- [16] Zimmermann S, Urbassek HM. *Nucl Instrum Methods B* 2005;228:75.
- [17] Postawa Z, Czerwiński B, Szewczyk M, Smiley EJ, Winograd N, Garrison BJ. *Anal Chem* 2003;75:4402.
- [18] Postawa Z, Czerwiński B, Szewczyk M, Smiley EJ, Winograd N, Garrison BJ. *J Phys Chem B* 2004;108:7831.
- [19] Postawa Z, Czerwiński B, Winograd N, Garrison BJ. *J Phys Chem B* 2005;109:11973.
- [20] Czerwiński B, Delcorte A, Garrison BJ, Samson B, Winograd N, Postawa Z. *Appl Surf Sci*, in press.
- [21] Garrison BJ. In: Vickerman JC, Briggs D, editors. *TOF-SIMS: surface analysis by mass spectrometry*. Manchester: IM Publications and Surface Spectra Limited; 2001. p. 223.
- [22] Kelchner CL, Halstead DM, Perkins LS, Wallace AE, Deprieto AE. *Surf Sci* 1994;310:425.
- [23] Stuart SJ, Tutein AB, Harrison JA. *J Chem Phys* 2000;112:6472.
- [24] Liu KSS, Yong CW, Garrison BJ, Vickerman JC. *J Phys Chem B* 1999;103:3195.
- [25] Animations of the sputtering process can be found at: <http://users.uj.edu.pl/~ufpostaw/animations.htm>
- [26] Delcorte A, Vanden Eynde X, Bertrand P, Vickerman JC, Garrison BJ. *J Phys Chem B* 2000;104:2673.
- [27] Hautman J, Klein ML. *J Chem Phys* 1989;91:4994.
- [28] Marrink SJ, Mark AEJ. *Am Chem Soc* 2003;125:15233.
- [29] Zhigilei LV, Leveugle E, Garrison BJ, Yingling YG, Zeifman MI. *Chem Rev* 2003;103:321.
- [30] Smiley EJ, Postawa Z, Wojciechowski IA, Winograd N, Garrison BJ. *Appl Surf Science*, in press.